AD-755 546

MAGNETIC BUBBLE MATERIALS

Jerry W. Moody, et al

Monsanto Research Corporation

Prepared for:

Advanced Research Projects Agency

11 February 1973

MRC-SL-354

SEMI-ANNUAL TECHNICAL REPORT

MAGNETIC BUBBLE MATERIALS

Monsanto Research Corporation
St. Louis, Missouri 63166

Jerry W. Moody, Robert M. Sandfort, and Roger W. Shaw

Contract No. DAAH01-72-C-1098

Distribution of this document is unlimited

ARPA Support Office
Research, Development, Engineering,
and Missile Systems Laboratory
U.S. Army Missile Command
Redstone Arsenal, Alabama

Sponsored by:
Advanced Research Projects Agency
ARPA Order Nr. 1809

UNCLASSIFIED

Security Classification

DOCUMENT CONTROL DATA - R & D

(Security classification of title, body of abstract and indexing annotation must be entered when the overall report is classified)

1. ORIGINATING ACTIVITY (Corporate author) Monsanto Research Corporation 800 North Lindbergh Boulevard St. Louis, Missouri 63166	2a. REPORT SECURITY CLASSIFICATION UNCLASSIFIED 2b. GROUP

3. REPORT TITLE

MAGNETIC BUBBLE MATERIALS

4. DESCRIPTIVE NOTES (Type of report and inclusive dates)

Semi-Annual Tech. Report (12 July, 1972 thru 11 January, 1973)

5. AUTHOR(S) (First name, middle initial, last name)

Jerry W. Moody
Robert M. Sandfort
Roger W. Shaw

6. REPORT DATE February 11, 1973	7a. TOTAL NO. OF PAGES 71	7b. NO. OF REFS 25
8a. CONTRACT OR GRANT NO. DAAH01-72-C-1098 b. PROJECT NO. ARPA Order No. 1999-72 c. d.	9a. ORIGINATOR'S REPORT NUMBER(S) MRC-SL-354 9b. OTHER REPORT NO(S) (Any other numbers that may be assigned this report)	

10. DISTRIBUTION STATEMENT

Distribution of this document unlimited

11. SUPPLEMENTARY NOTES Details of illustrations in this document may be better studied on microfiche.	12. SPONSORING MILITARY ACTIVITY Advanced Research Project Agency Washington, D. C.

13. ABSTRACT

This semi-annual technical report on the project "Magnetic Bubble Materials Phase II", Contract No. DAAH01-72-C-1098 covers the period 12 July, 1972 through 11 January, 1973.

The object of this project is to establish a reliable supply of high quality magnetic bubble materials to support the device work of various Department of Defense agencies. This work encompasses bulk, non-magnetic garnet crystal growth (for use as substrates), substrate polishing and preparation, liquid phase epitaxial growth of high performance magnetic garnet film compositions, chemical vapor deposition of Ga-YIG films, and the investigation of arc-plasma spraying as a technique for preparing magnetic bubble garnet films. Characterization data are given for materials delivered during this phase.

DD FORM 1 NOV 68 1473 REPLACES DD FORM 1473, 1 JAN 64, WHICH IS OBSOLETE FOR ARMY USE.

UNCLASSIFIED

Security Classification

14. KEY WORDS	LINK A		LINK B		LINK C	
	ROLE	WT	ROLE	WT	ROLE	WT
Magnetic bubble materials						
Magnetic garnets						
Gadolinium gallium garnets						
Crystal growth						
Liquid phase epitaxy						
Chemical vapor deposition						
Arc plasma spray						
Substrate preparation						
Rare-earth iron garnets						

SEMI-ANNUAL TECHNICAL REPORT

MAGNETIC BUBBLE MATERIALS

Monsanto Research Corporation
St. Louis, Missouri 63166

Jerry W. Moody, Robert M. Sandfort, and Roger W. Shaw

February 11, 1973

Contract No. DAAH01-72-C-1098

ARPA Support Office
Research, Development, Engineering
and Missile Systems Laboratory
U.S. Army Missile Command
Redstone Arsenal, Alabama

Sponsored by:
Advanced Research Projects Agency
ARPA Order No. 1999

iib

SUMMARY

This semi-annual technical report on the project "Magnetic Bubble Materials Phase II", Contract No. DAAH01-72-C-1098 covers the period 12 July, 1972 through 11 January, 1973.

The object of this project is to establish a reliable supply of high quality magnetic bubble materials to support the device work of various Department of Defense Agencies. This work encompasses bulk, non-magnetic garnet crystal growth (for use as substrates), substrate polishing and preparation, liquid phase epitaxial growth of high performance magnetic garnet film compositions, chemical vapor deposition of Ga-YIG films, and the investigation of arc-plasma spraying as a technique for preparing magnetic bubble garnet films.

Bulk, single crystal boules of $Gd_3 Ga_5 O_{12}$, $Sm_3 Ga_5 O_{12}$, and $Gd_{2.6} Y_{0.4} Ga_5 O_{12}$ were grown by the Czochralski technique during the contract period. Crystals of $Gd_3 Ga_5 O_{12}$ essentially free from the highly strained core region and with an acceptably low defect density were grown.

Epitaxial films of two different compositions were grown by LPE on {111} $Gd_3 Ga_5 O_{12}$ from a $PbO-B_2O_3$ solvent solution. A slightly different "dipping" arrangement, axial rotation of a horizontally held substrate, was implemented during this contract period. This technique resulted in significant improvement in film thickness uniformity. Growth conditions are presented.

Work was carried out on chemical vapor deposition (CVD) of YIG and Ga-YIG in the early months of this contract period, but it became clear that the objective of the contract, to supply device quality layers to ARPA, could better be met by LPE growth than CVD growth. With the consent of the project monitor, all CVD work was terminated.

Investigation of arc-plasma spraying as a technique for preparing magnetic bubble garnet films was undertaken during this contract period. The implementation of this method and the results obtained are presented. One magnetic garnet film composition was prepared by this technique.

Characterization of bubble materials was broadened during this phase of the contract to include temperature coefficient of characteristic length and magnetization measurements as well as compensation point determinations. Temperature data for all samples delivered to ARPA under the first phase of this program and those delivered during this reporting period are presented.

TABLE OF CONTENTS

LIST OF TABLES

LIST OF FIGURES

1. INTRODUCTION

During the first six months of this contract Monsanto has grown garnet materials by four different techniques; bulk, non-magnetic substrate crystals by Czochralski, and magnetic garnet thin films by liquid phase epitaxy, (LPE), chemical vapor deposition (CVD), and arc plasma spraying (APS). The Czochralski bulk crystal work, which is discussed in section 2 of this report, had as its primary goal the growth of low defect crystals of GGG which were free of the highly strained core region. Growth conditions were established for the 25 kw puller which achieved this g Boules were grown which had less than 10 defects per square centimeter and a nearly strain-free core. More importantly, the interrelated parameters of rotation rate, crucible size, crystal size, pull rate, furnace geometry and growth atmosphere are felt to be more fully understood in terms of ultimate boule quality.

In addition to GGG, crystals of yttrium substituted $Gd_3 Ga_5 O_{12}$ and $Sm_3 Ga_5 O_{12}$ were grown. The impetus for the mixed rare-earth garnet material growth was the need for a suitable substrate on which to deposit Ga-YIG by CVD. Boules of the desired composition, $Y_{0.6}Gd_{7.4}Ga_5O_{12}$ were grown successfully, although not of as high quality as GGG, and several substrate slices were delivered three months into the contract period.

Crystals of $Sm_3 Ga_5 O_{12}$ were also grown successfully although, again of poorer quality than GGG. It is felt that a need may arise for a substrate having a larger lattice constant than GGG, possibly in connection with the

development of a low Ga-containing iron garnet which supports sub-micron bubbles. This work is also discussed in section 2.

A rather important refinement of the LPE "dipping" technique was implemented during this report period, that of axial rotation of a horizontal substrate. Significant improvement in thickness uniformity was achieved with this method. This and other modifications and improvements of the LPE work are reported in section 4 of this report. Two compositions of LPE-grown films were delivered in the first six months of this contract phase; both compositions having better temperature characteristics than previously delivered material. This reflects Monsanto's and ARPA's interest in the development of a more temperature stable composition which retains other desirable features of garnet films delivered previously.

The CVD work carried out primarily in the first part of the report period is discussed in section 5. The primary emphasis of this work was to grow Ga-YIG on substrates of yttrium substituted GGG. However, it was clear that the object of the program, to deliver device quality bubble films to ARPA, would be achieved better by LPE than CVD. This, and a meeting of AGED in Washington in September, led to a recommendation by Monsanto, and an affirmative decision by the contract monitor to terminate all CVD work.

The investigation of arc-plasma spraying as a means for preparing films of bubble garnet material centered on a two-step procedure in which a polycrystalline film of garnet plus $PbO\text{-}B_2O_3$ solvent is sprayed on a GGG substrate which is subsequently heated to above the liquidus temperature and

cooled so as to form a single crystal film. This work is discussed in section 6, and characterization data given on the samples delivered to ARPA.

Improvements in and extensions of the material characterization techniques employed at Monsanto which were implemented during this report period are discussed in section 7. The primary emphasis was on developing adequate means to measure the temperature characteristics of bubble materials. The data obtained with these techniques are felt to be very illustrative of the temperature instability problems associated with previously delivered compositions, and very useful in attempting to improve the temperature characteristics of future compositions.

2. BULK CRYSTAL GROWTH

2.1 Introduction

The substrate most commonly used for the epitaxial growth of bubble domain garnet films is $Gd_3 Ga_5 O_{12}$. The lattice constant of this material matches that of a large number of magnetic garnet compositions, and methods of growth resulting in virtually perfect crystals of $Gd_3 Ga_5 O_{12}$ have been developed. This substrate has been used exclusively in this work to date. However, bulk crystals of other gallium garnets, as candidate substrate materials, have been grown on this program.

Bulk crystals of the rare-earth gallium garnets are conveniently grown by the Czochralski method. The growth of $Gd_3 Ga_5 O_{12}$ by the Czochralski method has been described in a previous report[1] and in the literature[2, 3]. Under proper conditions, virtually perfect crystals of $Gd_3 Ga_5 O_{12}$ can be grown; however certain types of defects are not uncommon. The origin of these defects and means of eliminating them were discussed in detail previously[1]. As a brief review, the most common defects and their causes are listed in Table 1.

During Phase I of this program conditions were established for growing crystals of $Gd_3 Ga_5 O_{12}$ which were essentially free of dislocations and inclusions. However, the crystals usually contained a highly strained core and growth striations. Part of the effort during this part of the program was directed toward eliminating these troublesome defects. In addition, the growth of rare-earth gallium garnets other than $Gd_3 Ga_5 O_{12}$ was investigated.

TABLE I

Common Defects in $Gd_3 Ga_5 O_{12}$

	Defect	Causes
1.	Inclusions	Improper oxygen over pressure or melt not in equilibrium with atmosphere
2.	Dislocations	Poor diameter control - large thermal gradients, high crystallization rate
3.	Coring (strains)	Non-planar growth interface
4.	Growth striations	Low thermal gradients - stoichiometric variations - high crystallization rate

2.2 Experimental

2.2.1 Apparatus and Materials

The garnet crystal growth furnaces used in this work were described in detail previously[1]. Essentially, the furnace consists of an inner stabilized ZrO_2 tube and an outer wall of fused silica. The inner tube is both lined and wrapped with Zircar* felt. The heat source is an iridium crucible which acts as a susceptor of RF power coupled inductively from water cooled coils wound around the outside furnace liner. The iridium crucible is supported upon a ZrO_2 pedestal. If growth in gases other than air is desired, these gases can be introduced through a port in a steel base plate and can flow out around the steel pull rod at the top of the furnace. The seed is tied to an Al_2O_3 seed holder with Pt + 13% Rh wire.

Although both a 10 kw and a 25 kw RF generator are available, only the 25 kw generator was used in this phase of the work. Iridium crucibles of two sizes were used: 1-1/4 inch I.D. x 1-1/4 inch high and 1-1/2 inch I.D. x 1-1/2 inch high.

The starting charges were usually prepared by mixing the appropriate oxide powders of 99.99% purity, in stoichiometric proportion. Occasionally, the tail-end or portions of previously grown crystals were used. Comparable results were obtained in both cases. The crucibles were usually charged to about 3/4 of capacity.

---

*Zircar is a trade-name of the Union Carbide Corporation.

2.2.2 Crystal Growth and Evaluation

All the garnet crystals prepared on this program were grown on seeds oriented along the < 111 > direction. Pull rates of 4-8 mm/hr were used. The rotation rate was varied from 10 rpm to 75 rpm. The crystals were grown in an O_2 - N_2 atmosphere with the O_2 concentration varied from about 2 to 5 percent by volume. Total gas flow rates of 1200-1300 ml/min were used. The diameter of the crystal was usually kept to about one half the diameter of the crucible used in an effort to reduce thermal strains.

After growth, the ends of the crystals were cut off perpendicular to the growth axis. The ends were then polished flat and parallel and the interior of the crystals was examined visually for cracks, inclusions and voids. The extent and distribution of elastic strain was determined by examining the crystal between crossed polarizers.

If the boule appeared to be sound and free of inclusions, then the orientation of the crystal was determined by back-reflection X-ray procedures and (111) wafers were sliced from the front, middle and rear of the crystal. Certain of the wafers were used for precise lattice constant measurements. Others were polished and then etched for 5 minutes in orthophosphoric acid at 160-170°C. These wafers were then examined microscopically for dislocations, inclusions and growth striations. The wafers were examined in both transmitted and reflected light. The differential interference microscope was particularly valuable in studying the "core" and growth striations in the etched wafers.

2.3 Results and Discussion

2.3.1 Growth of Core-Free $Gd_3 Ga_5 O_{12}$

A highly strained central core is one of the most characteristic features of Czochralski grown rare-earth garnets. This strained core is associated with the formation of crystal facets on a non-planar solid/liquid interface during crystal growth. In the case of $Gd_3 Ga_5 O_{12}$, Glass[4] has shown that the lattice parameter of the faceted region is 0.001-0.002 Å larger than that of the unfaceted region. (Glass attributes the lattice parameter difference to a compositional difference between the faceted and unfaceted regions and he reasons that the unfaceted region contains excess Ga substituting for Gd on a dodecahedral sites while the faceted regions are more stoichiometric.) Lattice parameter differences of as much as 0.001 Å in the substrate can have a pronounced effect on the magnetic properties (anisotropy, domain diameter, etc.) of epitaxial bubble domain films. Therefore, "core-free" substrates are preferred (perhaps required) for device quality magnetic films.

Since the core is associated with a non-planar growth interface, it can be eliminated by establishing and maintaining a flat solid/liquid interface during crystal growth. This is conveniently done by adjusting the rotation rate of the growing crystal[5]. In previous work[1], the core in $Gd_3 Ga_5 O_{12}$ was eliminated by increasing the normal rotation rate (about 10-20 rpm) to 50-60 rpm. However, the crystals contained an unacceptable density of dislocations. To minimize the occurrence of dislocations, it was found

necessary to reduce the normal pull rate. The maximum pull rate that can be employed decreases as the rotation rate is increased. In this work satisfactory results have been obtained using a rotation rate of 50 rpm and a pull rate of 3.2 mm/hr.

The effect of rotation and pull rates on the strains in Czochralski grown $Gd_3 Ga_5 O_{12}$ crystals is illustrated in Figure 1 in which representative crystals are photographed between crossed-polarizers. The highly strained core is obvious in Crystal 5547 while the strains are not as severe and are more uniformly distributed in Crystal 5517. The dislocation density in both crystals is at an acceptable level.

Experience indicates that the optimum rotation and pull rates for the growth of $Gd_3 Ga_5 O_{12}$ depend upon the particular furnace arrangement being used. The amount of insulation in the furnace, thermal gradients, size of crystal and crucible — all must be considered when growing the crystal. Therefore, it is not possible to specify particular rotation and pull rates that can be used in general. These conditions must be established for each furnace arrangement.

2.3.2 Growth of $Sm_3 Ga_5 O_{12}$

Although $Gd_3 Ga_5 O_{12}$ has been the "workhorse" substrate for garnet bubble films, other non-magnetic garnets are of interest as candidate substrates. One such garnet is $Sm_3 Ga_5 O_{12}$ which has a lattice parameter, a_0, of 12.432. Such a substrate is compatible with the temperature stable compositions of the Sm-Y and Eu-Y magnetic garnet systems as well as other

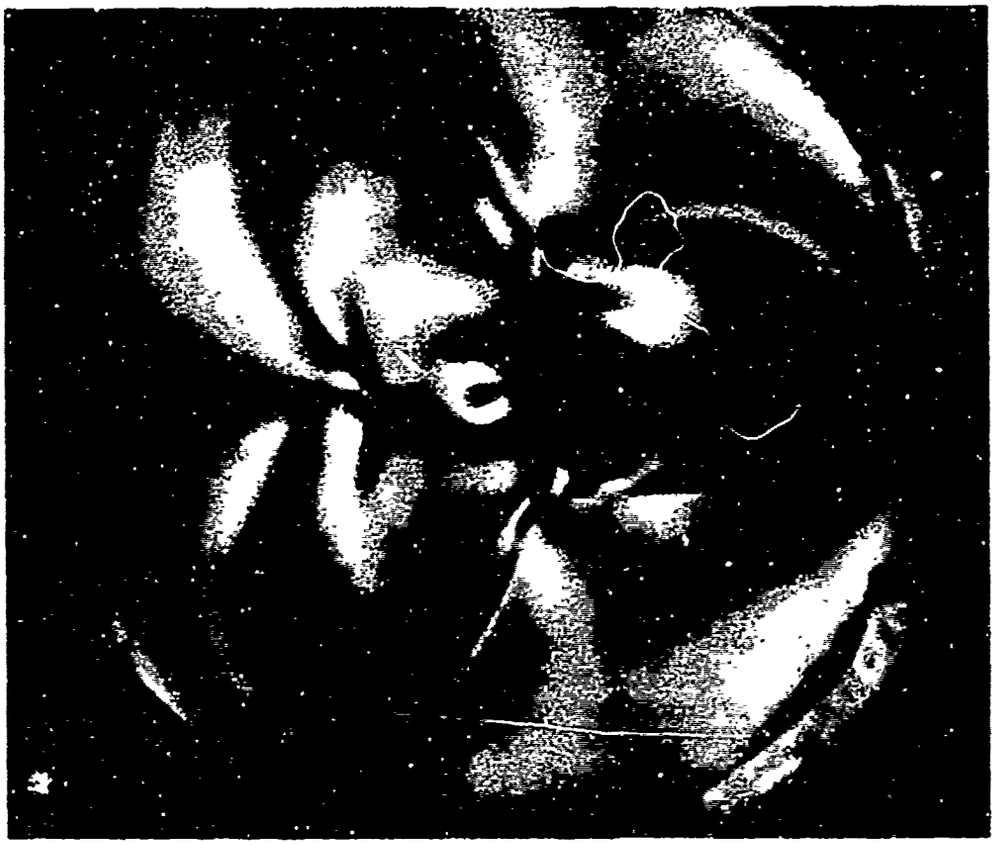

Rotation rate 20 rpm
Pull rate 6.4 mm/hr
Dislocation density $<10/cm^2$
Crystal diameter 17 mm

Figure 1A. Effect of Rotation Rate and Pull Rate on Strains in $Gd_3Ga_5O_{12}$: Crystal 5547

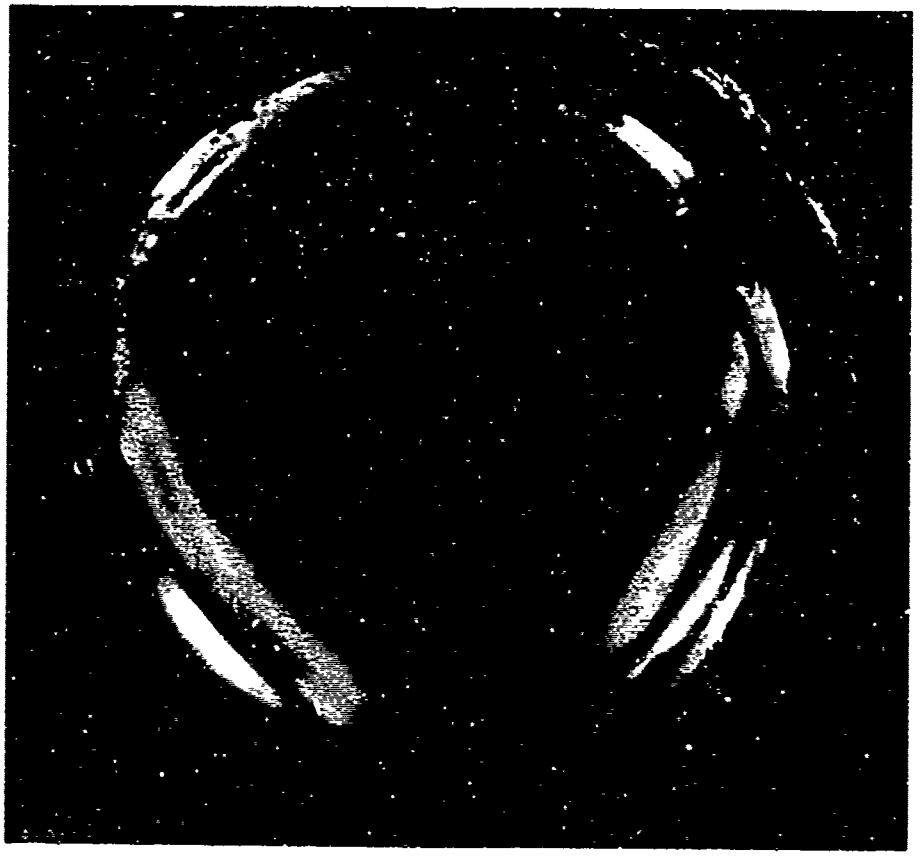

Rotation rate 50 rpm
Pull rate 3.2 mm/hr
Dislocation density $<10/cm^2$
Crystal diameter 16 mm

Figure 1B. Effect of Rotation Rate and Pull Rate on Strains in $Gd_3Ga_5O_{12}$: Crystal 5517

magnetic garnets. It might be particularly useful for magnetic films supporting sub-micron bubbles which contain only small amounts of Ga or Al, and has been used for such compositions in the Eu-Y system[6].

Several boules of $Sm_3 Ga_5 O_{12}$ have been pulled under conditions quite similar to those used for $Gd_3 Ga_5 O_{12}$. However, low defect densities and good diameter control has not been achieved as yet and work on the growth of $Sm_3 Ga_5 O_{12}$ will be continued.

2.3.3 Growth of Mixed Garnet Crystals

A substrate suitable for the epitaxial growth of $Y_3 Fe_{5-x} Ga_x O_{12}$ was of particular interest to this program. The lattice parameter of the nominal composition $Y_3 Fe_4 Ga_1 O_{12}$ is estimated to be 12.362. Since films of this composition must be in tension to exhibit magnetic anisotropy a substrate with a lattice parameter of about 12.370 was desired. The lattice parameters of the rare-earth gallium garnets range from 12.188 Å for $Lu_3 Ga_5 O_{12}$ to 12.570 Å for $Pr_3 Ga_5 O_{12}$. Since the rare-earth garnets tend to form solid solutions, any lattice parameter between these and points can be obtained by preparing a mixed crystal of appropriate rare-earth gallium garnets. $Gd_3 Ga_5 O_{12}$ and $Y_3 Ga_5 O_{12}$ were selected as end members to provide mixed crystal having the desired lattice parameter. The desired composition, $Gd_{2.6} Y_{0.4} Ga_5 O_{12}$, was arrived at by applying Vegard's law.

Two crystals of the nominal composition $Gd_{2.6} Y_{0.4} Ga_5 O_{12}$ were pulled at 3.2 mm/hr. One crystal was grown at a rotation rate of 10 rpm, the other at 20 rpm. Similar results were obtained in both cases. A strained central

core was obvious in both crystals. The lattice parameter of both crystals was 12.370 ± 0.001 Å which agrees with the lattice parameter estimated from Vegard's law. Polished wafers from the crystals were supplied to the Sponsor.

3. SUBSTRATE PREPARATION

Many of the defects found in present day epitaxial garnet films can be traced directly to improper substrate preparation and handling. A lapping, polishing and cleaning procedure for $Gd_3 Ga_5 O_{12}$ that produces an excellent surface for epitaxial growth was described in detail previously[1]. The same basic procedure, with two modifications, is now used to prepare substrate surfaces.

First, it was found that the intermediate lapping step with 0.3 μm $Al_2 O_3$ on an AB Texmet* lap is not necessary. The substrates can be taken directly from the 3 μm $Al_2 O_3$ lapping step to the Syton** polish provided at least 25 μm of surface are removed on the Syton-flooded lap.

Second, a more concentrated solution of Syton is now used. The Syton is now diluted 25 parts Syton/10 parts deionized water. This results in a slightly higher removal rate than was obtained with the 20/15 dilution used previously.

The effect of both of these modifications of the polishing procedure is to reduce the time required to prepare the substrate for epitaxial growth. Still, the most time-consuming, and the most important step of the procedure is the final polish with Syton. Experience indicates that at least 25 μm must be removed by the final polish to obtain, reproducibly, a surface free of work damage.

---

* Texmet is a trade-name of Buehler, Ltd.

** Syton is a trade-name of Monsanto Company.

The material removal rate achieved on the Syton-flooded Corfam*** lap depends on a number of factors:

1. Concentration of Syton
2. Temperature
3. Applied Force
4. Total surface area being polished
5. Age, or condition, of the Corfam lap

In general, the removal rate increases with the first three factors listed above and decrease with the last two. The usual removal rate used at Monsanto is 15-20 μm/hr. However, the final condition of the substrate surface does not depend on the removal rate used but on the total amount of garnet removed.

*** Corfam is a trade-name of Dupont.

4. LIQUID PHASE EPITAXY

4.1 Introduction

Six different film compositions were supplied to the Sponsor during the first phase of this program:

1. $Eu_{0.6}\ Er_{2.4}\ Fe_{4.4}\ Ga_{0.6}\ O_{12}$
2. $Gd_{0.8}\ Er_{2.2}\ Fe_{4.6}\ Ga_{0.4}\ O_{12}$
3. $Gd_{0.5}\ Y_{2.5}\ Fe_{4}\ Ga_{1}\ O_{12}$
4. $Gd_{1}\ Yb_{0.9}\ Y_{1.1}\ Fe_{4.2}\ Ga_{0.8}\ O_{12}$
5. $Gd_{0.44}\ La_{0.04}\ Y_{2.52}\ Fe_{4.0}\ Ga_{1}\ O_{12}$
6. $Gd_{1.1}\ Tm_{0.9}\ Y_{1}\ Fe_{4.3}\ Ga_{0.7}\ O_{12}$

Although all these compositions were tailored to support stable 5 - 6 μm bubble domains, they exhibit a wide range and variety of magnetic properties. The anisotropy of compositions 1 and 2 is primarily growth induced; that of composition 3 is stress-induced, while that of compositions 4, 5, and 6 is probably both growth- and stress-induced. The magnitude of the anisotropies range from about 220 Oe (for composition 3) to 3800 Oe (composition 1) while domain mobilities range from less than 100 cm/sec/Oe (composition 1) to over 600 cm/sec/Oe (composition 4).

Because of their range of properties these first compositions were valuable for basic property studies and preliminary device work. However, none of the compositions possessed the combination of high mobility and temperature stability that is required for a practical device. Therefore, attention has now been directed toward developing compositions with adequate

temperature stability which also have the desirable features of several of the compositions in the above list. A brief review of compositional properties felt to be important is in order.

4.1.1 Guidelines for Composition Development

In attempting to develop an optimum magnetic garnet film composition for use in bubble devices, one is guided and constrained primarily by four factors:

1. The lattice constant of the composition must match the lattice constant of GGG within about ± 0.01 Å. In addition, this lattice match must occur at a non-magnetic diluent ion (Ga, Al) concentration at which the desired bubble diameter is obtained.
2. Rare-earth ions which exhibit narrow ferromagnetic resonance linewidths as pure iron garnets must be used predominantly to obtain high domain wall velocities.
3. Temperature stability of ℓ must be maintained by eliminating those rare-earth ions which, as pure iron garnets, have high temperature compensation points.
4. The composition must exhibit growth-induced anisotropy normal to the film plane. The magnitude of the anisotropy field must be between 1000 Oe and 2000 Oe.

The ramifications of most of these factors are well understood and have been discussed in detail in the literature[7,8]. However, guidelines for grooming a material for superior temperature stability and at the same time

maintaining other desirable properties has not received sufficient emphasis and the discussion here will center on improving temperature stability.

4.1.1.1 Temperature Stability

One of the more important considerations in the search for an acceptable magnetic garnet film composition for bubble devices is the variation of the operating bubble diameter and bias field with temperature. Hagedorn, et al[9] have given the total variations of these quantities, and Smith and Anderson[10] have eliminated the thickness variation (since thickness doesn't change with temperature) from Hagedorn's results to obtain only the temperature variations. These are:

$$\frac{\Delta H}{H} = \frac{\Delta M_s}{M_s} - C_1 \frac{\Delta \ell}{\ell} ,$$

$$\frac{\Delta d}{d} = C_2 \frac{\Delta \ell}{\ell} ,$$

where C_1 and C_2 are thickness dependent constants, and

$$\frac{\Delta \ell}{\ell} = \frac{\Delta \sigma_w}{\sigma_w} - \frac{2 \Delta M_s}{M_s}$$

These equations actually represent different design philosophies. The first condition, which points the way to achieving constant bias field as a function of temperature, has been more easily realizable in practice since it depends heavily on achieving a constant magnetization in a region about room temperature. This can be done by utilizing at least one rare-earth ion in the garnet formula which has a compensation point as a pure iron garnet. In a composition such as YGd GaIG, for example, YIG has no compensation point, and GdIG has the highest temperature compensation point of all the rare-earth

iron garnets. Therefore, if a sufficient amount of Gd^{3+} is substituted into YGaIG, it is possible to obtain a composition in which the compensation temperature and the Neel temperature are displaced equally about room temperature resulting in a fairly flat region of magnetization at room temperature, and hence a constant operating bias.

The second expression indicates what is necessary to achieve a temperature independent bubble diameter. This appears to be the most useful temperature criterion for bubble devices, but has also been more difficult to achieve to date. To within a constant, a temperature independent bubble diameter can be obtained by grooming the material for constant characteristic length. This can be done by balancing the temperature variation of wall energy against the temperature variation of magnetization. The temperature variation of wall energy is dominated by the anisotropy constant which in all compositions measured to date decreases with increasing temperature. This behavior appears to hold both for growth induced and stress induced anisotropy. Since the wall energy is a decreasing function of temperature, the magnetization must also decrease with temperature in such a way as to keep ℓ constant. YIG, as well as all pure rare earth iron garnets which do not have compensation points exhibit this behavior. Rare earth type ions which are suitable in this respect are Lu^{3+}, Y^{3+}, Eu^{3+}, Sm^{3+}, Nd^{3+}, Pr^{3+}, and La^{3+}, however, the last three ions are too large to form pure iron garnets. YbIG and TmIG have low temperature compensation points, so that their characteristic magnetization versus temperature behavior is suitable enough for very limited substitutions of Yb^{3+} and Tm^{3+} to be of interest.

However, when an ion which displays a compensation point as a pure iron garnet, such as Gd^{3+}, is substituted into a composition which has no compensation point, such as YGaIG, it introduces a compensation point into this composition. In addition, the effect of non-magnetic Ga^{3+} ions is to push the compensation point to higher temperatures with increasing Ga concentration. As a result, it is very difficult to maintain the proper negative temperature coefficient of $4\pi M_s$ in compositions having a high temperature compensation point. The worst offending ion in this regard is Gd^{3+} which is a quite desirable ion from the standpoint of wall mobility. Gd^{3+} raises the compensation point of $M_yY_{3-y}Ga_xFe_{5-x}O_{12}$ more per atom than any other rare earth. This effect, and the fact that Gd substituted YGaIG films display in-plane growth induced anisotropy have led to an examination of Eu^{3+} substituted Y(GaAl)IG compositions instead of Gd^{3+}. Eu^{3+} has no compensation point as a pure iron garnet which improves the temperature stability of the characteristic length, and, in addition leads to growth induced anisotropy of the proper magnitude normal to the {111} plane in $Eu_x\ Y_{3-x}\ (Ga,\ Al)_y\ Fe_{5-y}\ O_{12}$ films. The FMR linewidth of pure EuIG is the next narrowest after GdIG, so that one expects to achieve nearly as high domain wall mobilities in Eu^{3+} — containing YGaIG compositions as in Gd^{3+} — containing YGaIG layers if the Eu^{3+} concentration is kept sufficiently low. This will be discussed further in the sections on characterization and results and conclusion.

4.2 Experimental

4.2.1 Thickness Uniformity

The growth of magnetic garnet films from undisturbed, supercooled $PbO-B_2O_3$ solutions has been described previously[1]. Recently, the procedures discussed there were modified to improve film thickness uniformity. The modification consisted of implementing growth in a horizontal plane with axial rotation as described by Giess, et al[11]. The same type of platinum wire - Al_2O_3 rod substrate holder as used previously is still used except that three wires are required to hold the substrate in a horizontal plane.

Axial rotation affects the thickness of the diffusion boundary layer at the film solution interface. Garnet components must diffuse from the solution across this layer to be incorporated into the growing film. Giess[11] found growth rates to be proportional to the square-root of the rotation rate at constant supercooling. Similar results have been obtained in this work.

Axial rotation also tends to reduce the thermal gradients which might exist in an unstirred solution and, thereby, promotes uniform film growth across the substrate. The thickness uniformity which can be achieved by this method is illustrated in Figure 2. This photograph was made in monochromatic light where each fringe corresponds to a thickness difference of 0.122 μm. Except for the very edge and the small areas covered by the platinum wire holder, the thickness of the film is 7.94 ± 0.06 μm. This degree of thickness uniformity is obtained reproducibly on the largest substrates (25 - 30 μm) which are commercially available at present.

Figure 2. Thickness Uniformity of LPE Film Grown with Axial Rotation

4.2.2 Growth Parameters for Eu-Y Compositions

During this report period two compositions of the Eu-Y magnetic garnet system were delivered to ARPA. The Eu/Y concentration ratios in the two compositions were widely different but both were tailored to support 6 μm bubbles. Aluminum, rather than Ga, was used as the non-magnetic diluent in the Eu-rich composition. The solution compositions and conditions of growth are given in Tables II and III. The $Eu_2\ Y_1\ Fe_{4.1}\ Al_{0.9}\ O_{12}$ films were grown without rotation.

As yet accurate distribution coefficients have not been determined for these compositions. Therefore, the film compositions given must be regarded as approximate. It is very probable that the $Eu_2\ Y_1\ Fe_{4.1}\ Al_{0.9}\ O_{12}$ films contain somewhat more Al than is indicated in the nominal formula.

4.3 Results and Discussion

The magnetic properties of the samples delivered during this report period are summarized in Table IV. The most striking difference in the properties of the two compositions is in the mobility. The mobility of most of the Eu-rich films is about one third that of the Y-rich films. The temperature coefficients of characteristic length are similar for the two compositions. The observations suggest that the most practical compositions would contain no more Eu than is necessary to achieve temperature stability and the desired growth-induced anisotropy.

The coercivity of the Eu-Y compositions is of interest. The values, 0.33 to 0.54 Oe, given in Table IV are relatively high for the garnets. Such high values appear to be characteristic of Eu-containing compositions.

TABLE II

Growth Parameters for $Eu_2\ Y_1\ Fe_{4.1}\ Al_{0.9}\ O_{12}$

Solution Composition

Compound	Mole Percent
PbO	87.17
B_2O_3	5.67
Eu_2O_3	0.40
Y_2O_3	0.20
Fe_2O_3	5.97
Al_2O_3	0.59

Saturation Temperature : $\approx$ 945°C

Growth Temperature : 924

Growth Rate : $\approx$ 0.12 μm/min.

TABLE III

Growth Parameters for $Eu_{0.6}\ Y_{2.4}\ Fe_{3.74}\ Ga_{1.26}\ O_{12}$

Solution Composition

Compound	Mole Percent
PbO	86.09
B_2O_3	5.52
Eu_2O_3	0.12
Y_2O_3	0.48
Fe_2O_3	6.81
Al_2O_3	0.98

Saturation Temperature : ≈965°C

Growth Temperature : 938

Rotation Rate : 100 RPM

Growth Rate : ≈0.59 μm/min.

TABLE IV

CHARACTERIZATION DATA OF BUBBLE FILMS

Nominal Composition	Sample Number	h (μm)	ℓ (μm)	4πMs (G)	σ_w (ergs/cm²)	Hc (Oe)	H_A (Oe)	μ (cm/sec Oe)	H_{s-b} (Oe)	d_{s-b} (μm)	H_s (Oe)	d_s (μm)	T_N (K)	T_c (K)	$\frac{1}{\ell}\frac{d\ell}{dT}$ (K^{-1})	$\frac{1}{M_s}\frac{dM_s}{dT}$ (K^{-1})
$Eu_3Y_1Fe_{4.1}Al_{0.9}O_{12}$	EuY-1	5.17	0.76	152	0.14	.44	1600	7*	48	11	70	2	404	< 77	-.0066	-.0028
$Eu_3Y_1Fe_{4.1}Al_{0.9}O_{12}$	EuY-2	5.39	0.84	157	0.16	0.54	1707	54	49	10	70	2	402	< 77	-.0066	-.0028
$Eu_3Y_1Fe_{4.1}Al_{0.9}O_{12}$	EuY-3	5.10	0.83	155	0.16	0.46	1340	90	49	10	68	2	402	< 77	-.0080	-.0023
$Eu_3Y_1Fe_{4.1}Al_{0.9}O_{12}$	EuY-4	4.08	0.84	143	0.14	0.54	1270	67	36	11	54	2	400	< 77	-.0080	-.0025
$Eu_3Y_1Fe_{4.1}Al_{0.9}O_{12}$	EuY-5	4.43	0.79	138	0.12	0.48	1228	67	38	10	57	2	402	< 77	-.0080	-.0025
$Eu_{0.6}Y_{2.4}Fe_{3.76}Ga_{1.24}O_{12}$	EuY-11	7.37	0.73	147	0.13	0.33	1180	210	59	9	79	3	396	< 77	-.0062	-.0030
$Eu_{0.6}Y_{2.4}Fe_{3.76}Ga_{1.24}O_{12}$	EuY-12	7.37	0.76	150	0.13	0.33	1180	210	61	8	79	3	396	< 77	-.0062	-.0030
$Eu_{0.6}Y_{2.4}Fe_{3.76}Ga_{1.24}O_{12}$	EuY-13	7.13	0.73	144	0.12	0.33	1180	210	60	10	78	2	396	< 77	-.0062	-.0030
$Eu_{0.6}Y_{2.4}Fe_{3.76}Ga_{1.24}O_{12}$	EuY-14	7.25	0.76	148	0.13	0.33	1180	210	60	9	78	3	396	< 77	-.0062	-.0030
$Eu_{0.6}Y_{2.4}Fe_{3.76}Ga_{1.24}O_{12}$	EuY-15	7.25	0.71	147	0.12	0.33	1180	210	62	9	80	3	396	< 77	-.0062	-.0030

5. CHEMICAL VAPOR DEPOSITION

5.1 Introduction

Linares, et al[12, 13] were first to utilize vapor phase reactions to prepare epitaxial films of magnetic garnet. They deposited $Y_3 Fe_5 O_{12}$ on a variety of substrates, including a number of nonmagnetic garnets. The layers deposited on $Gd_3 Ga_5 O_{12}$ substrates were found to be highly perfect single crystal films. Subsequently, the process has been developed by a number of workers, most notably the group at North American Rockwell who have published a number of papers describing the chemical vapor deposition (CVD) of magnetic garnet films. Others who have contributed to the advancement of the art include Robinson, et al.[14], Stein[15], Ospresko and Pinch[16] and Taylor and Sadagopan[17]. Wehmeier[18] has considered the thermodynamic relations involved in the chemical transport of $Y_3 Fe_5 O_{12}$ with HCl.

The chemical vapor deposition of the magnetic garnets involves the reaction of the appropriate gaseous metal halides with oxygen and/or water vapor. The deposition of $Y_3 Fe_5 O_{12}$ may be considered as illustrative. Here the deposition reaction can be written:

$$3YCl_3\ (g) + 5FeCl_2\ (g) + 19/2\ H_2O\ (g) + 5/4\ O_2\ (g) \longrightarrow$$

$$Y_3 Fe_5 O_{12}\ (s) + 19HCl\ (g)$$

The metal chlorides can be used directly or formed, in situ, by the reaction of the metals and HCl.

Usually, the metal halides are evaporated into an inert carrier gas stream which transports them into a reaction zone where they are mixed with O_2/H_2O near a suitable substrate. The deposition temperature necessary to achieve smooth epitaxial growth of the garnet is about 1200°C Besides garnet, several other solids are stable at this temperature. These include Fe_2O_3, YOCl, Y_2O_3, and $YFeO_3$. All these compounds can form along with the garnet and contaminate the epitaxial layer. Under the most adverse conditions, garnet will not be formed at all. Dry HCl gas is usually introduced with the inert carrier gas to moderate the side reactions and the concentration of the reactants must be precisely adjusted to promote the formation of garnet at the expense of the other possible compounds.

All the magnetic epitaxial garnets prepared to date by CVD methods exhibit strain-induced anisotropy. It is doubtful whether the ion-ordering required for growth-induced anisotropy can be achieved at the elevated temperature (1200°C) necessary to promote epitaxial growth of garnet by CVD. Indeed, 1200°C is sufficient to quickly anneal out the anisotropy in most garnets which exhibit a magnetic superstructure. Thus, it appears that only stress-induced anisotropy will be achieved in compositions grown by CVD.

During this phase of the program, an investigation of the preparation of $Y_3Fe_5O_{12}$ and Ga substituted $Y_3Fe_5O_{12}$ was carried out.

5.2 Experimental

The CVD system used at Monsanto to deposit $Y_3 Fe_5 O_{12}$ films is shown in Figure 3. It consists of a quartz reactor mounted in a vertical, four-zone furnace. The temperature of each zone of the furnace is controlled independently. The YCl_3 and $FeCl_2$ are contained in Pt crucibles in the top of the reactor and maintained at about 1050°C and 750°C, respectively. The carrier gas (helium) and dry HCl are introduced at the top of the reactor and transport the halides downward into the reaction zone. Oxygen and water vapor along with additional helium are brought into the reaction zone through the second quartz tube. The substrates are mounted in the reaction zone on a rotating wedge-shape, quartz pedestal. The baffles in the reactor serve to isolate the temperature zones and promote mixing of the reactants. Typical deposition conditions are given in Table V. Epitaxial films about 2 microns thick are grown under these conditions.

To prepare Ga substituted $Y_3 Fe_5 O_{12}$, $GaCl_2$ is formed in the reactor by the reaction of gallium metal and HCl (g). The Ga metal is contained in a quartz crucible as is indicated in Figure 3. The amount of Ga which substitutes for Fe in the film was found to depend directly upon the mole ratio of Ga to Fe in the gaseous reactants.

The substitution of Ga for Fe in $Y_3 Fe_5 O_{12}$ results in a smaller unit cell and epitaxial films of Ga: $Y_3 Fe_5 O_{12}$ more than a few microns thick on $Gd_3 Ga_5 O_{12}$ substrates were invariably cracked. However, sound films were deposited on $Gd_{2.6} Y_{0.4} Ga_5 O_{12}$ substrates.

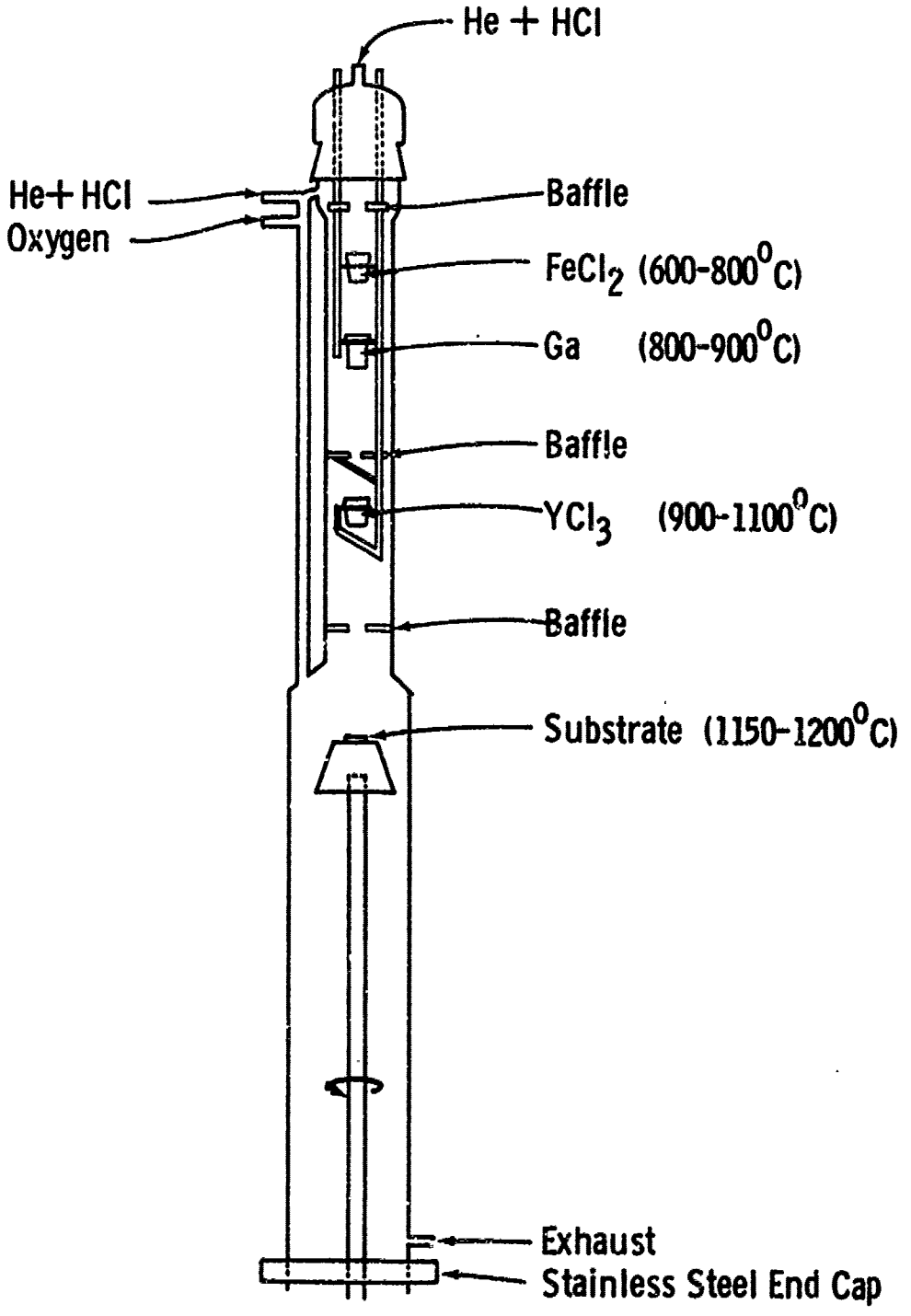

Figure 3. CVD Reactor

TABLE V

Conditions for the Preparation of $Y_3 Fe_5 O_{12}$ Films

$FeCl_2$ Temperature	750°C
YCl_3 Temperature	1100°C
Substrate Temperature	1180°C
$FeCl_2$ Transport Rate	1.3 gm/hr
YCl_3 Transport Rate	0.4 gm/hr
He Flow Rate (carrier gas)	800 cc/min.
He Flow Rate (oxygen diluent)	100 cc/min.
"Free" HCl	35 cc/min.
Oxygen Flow Rate	50 cc/min.
Deposition Time	2 hours

5.3 Results and Discussion

Some major problems were encountered in this work. These included slow growth rates and contamination of the epitaxial films by products of side reactions. However, the most serious problem was reproducing the material transport rates from run to run. Part of the problem could be ascribed to the difficulty of maintaining the chlorides in an anhydrous, oxygen-free condition.

The solution of these problems appeared to be formidable and it became apparent that the CVD process could not be controlled to the extent that the LPE process could during the contract period. It appeared that this opinion was also held by the majority of participants at the DOD seminar in Mangetic Bubble Technology held in Washington, D.C., September 27-28, 1972. Since the prime object of this program was to ensure delivery of device quality films to ARPA, Monsanto recommended that work on CVD be terminated and that LPE compositions be delivered instead of CVD compositions. ARPA accepted this recommendation and work on the CVD process was terminated at the end of October, 1972.

6. PLASMA SPRAYING

Plasma spraying was investigated to determine its potential to produce thin magnetic garnet films with superior or unique properties on substrates or to produce magnetic films with satisfactory characteristics at lower cost than traditional crystal growth processes. Two approaches were designated for study: (1) the conversion of plasma-sprayed polycrystalline garnet films into monocrystalline films; and (2) the direct fabrication of plasma-sprayed monocrystalline garnet films. The former method of converting sprayed films was studied during the first portion of this contract and results of this work are reported in this section.

6.1 Introduction

The two-step process for forming monocrystalline films consists of fabricating sprayed polycrystalline films containing garnet and flux and subsequently converting the deposits into monocrystalline garnet films by a thermal treatment.

First, a mixture of flux and oxides corresponding to the desired garnet composition are fused at elevated temperature and the resulting mass is cooled and converted into a powder for spraying. This particulate matter is then injected into a high-temperature streaming thermal plasma, formed by passing an inert gas through an electric arc, for controlled melting therein and for subsequent deposition onto an oriented non-magnetic substrate to form a polycrystalline film. The composite structure of film and substrate are then heated using a controlled temperature-time cycle and a monocrystalline epitaxial layer of magnetic garnet is formed on the non-magnetic monocrystalline substrate.

6.2 Experimental

6.2.1 Arc Plasma Spraying Station

Figure 4 is a schematic drawing of the arc plasma spraying (APS) apparatus. The spray torch is a device for forming a streaming thermal plasma and for injecting particulate matter for melting and spraying. The torch consists of two concentric water-cooled electrodes - a stick-type thoriated tungsten cathode located in the rear, and a nozzle-type copper anode located at the front.

In operation, a direct current electric arc is formed between the tip of the cathode and the inside wall of the anode. An inert arc gas, typically argon, is continuously passed through the arc for heating and ionization. The streaming thermal plasma thus formed is ejected from the nozzle resembling a flame. Particulate matter is transported from a powder feeder using a carrier gas and injected into the torch nozzle for heating in the plasma stream. Molten particles leaving the torch are directed against a substrate for collection, coalescence, and film formation.

Most films were sprayed inside a protective enclosure consisting of an extended pyrex tube connected to a bellows which in turn was connected to the front nozzle of the spray torch. The substrate was positioned within the tube and molten particles were deposited on the substrate in the usual manner. The protective enclosure served to minimize entrainment of airborne contaminants which, if collected on the sprayed deposit, could adversely affect film quality.

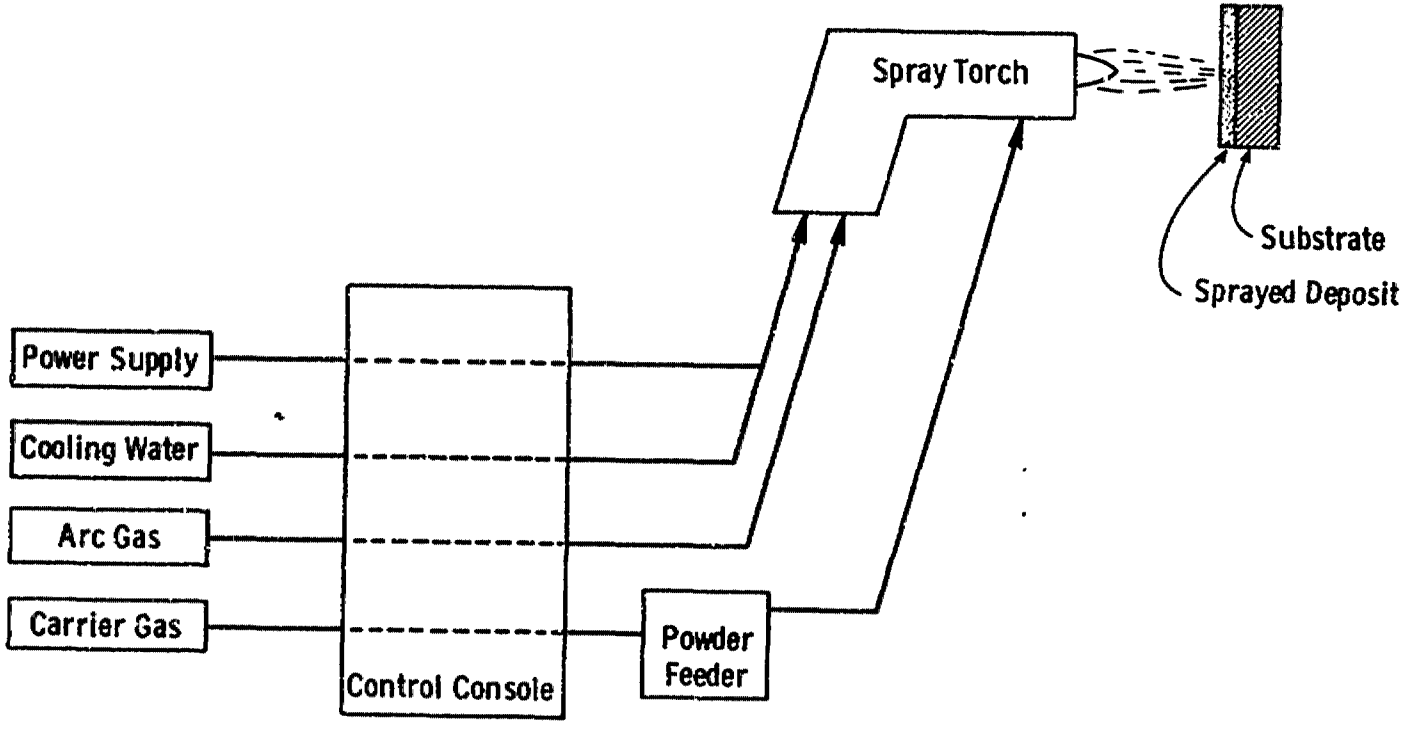

Figure 4. Schematic of Arc Plasma Spraying Process

After the prescribed deposition time in either the open or closed system, the spray torch was de-energized and the coated substrate was removed from its holder and readied for conversion.

6.2.2 Thermal Conversion Station

Figure 5 is a schematic drawing of the furnace used to convert plasma-sprayed polycrystalline garnet and flux coatings on GGG substrates into garnet single crystal epitaxial films. The furnace is capable of being tilted about a horizontal axis to enable the flux to be drained after conversion. During growth, the furnace is in a vertical position. An inner alumina tube, on which a molybdenum furnace winding is located, is situated inside of a larger alumina tube to create a sealed annular area in which hydrogen is passed to minimize winding degradation.

The platinum substrate holder is mounted securely to an alumina pedestal which is attached to a stainless steel tube that can be moved into and out of the furnace. During conversion, compressed air is slowly fed into the tube to reduce the temperature along the bottom of the substrate holder and maintain an oxidizing atmosphere inside of the furnace. The substrate temperature is monitored using a Pt/Pt-13%Rh, reference grade thermocouple which is in physical contact with the bottom of the platinum substrate holder. The furnace is normally preheated to the homogenization temperature and the pull tube, with substrate holder in place, is slowly moved into the furnace hot zone. After the required hold time, the temperature is reduced at a controlled programmed rate until the growth temperature is

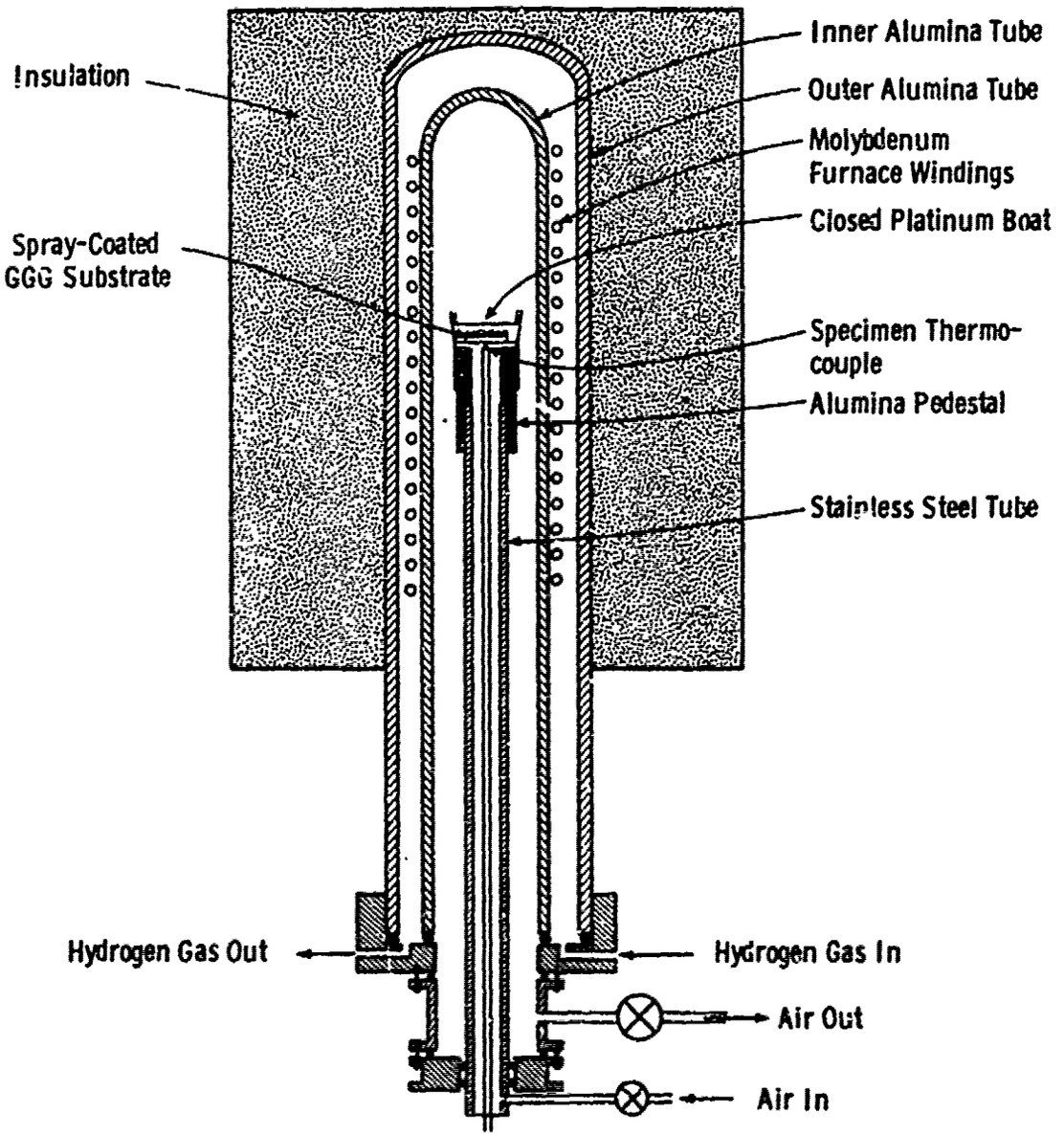

Figure 5. Schematic of Conversion Furnace

reached. After growth, the furnace is tilted, if desired, and the epitaxial film plus substrate is quickly cooled by pulling the holder out of the furnace.

6.2.3 Materials

Gadolinium oxide (Gd_2O_3), erbium oxide (Er_2O_3) and boron oxide (B_2O_3) were obtained from Research Inorganic/Organic Corporation and were 99.9%, 99.9% and 99.99% pure, respectively. Erbium oxide used in earlier runs was obtained from Alfa Inorganics Corporation and had a purity of 99.9%. Grade I iron oxide (Fe_2O_3), gallium oxide (Ga_2O_3) and lead oxide (PbO), manufactured by Johnson Matthey Chemicals Limited, were obtained from United Mineral and Chemical Corporation with a purity of 99.99%.

The individual oxides were weighed to four significant figures using an Ainsworth triple beam balance and subsequently blended for one hour. A typical powder mixture consisted of the following:

Component	Weight %
PbO	91.26
B_2O_3	1.83
Er_2O_3	0.90
Ga_2O_3	0.33
Gd_2O_3	0.31
Fe_2O_3	5.37

A homogeneous mixture of the oxides was obtained by forming a solution at high temperature. The solution was heated in a closed platinum crucible at

~ 1025°C for two hours and then quickly poured into a platinum boat. The resultant ingot was pulverized using a mill containing a tungsten carbide rotating blade to form a powder which, after sifting, was suitable for injection into the plasma spray torch.

The GGG substrates were all obtained with one side polished. Initially, high-defect GGG substrates were utilized and many early converted films displayed etch pits, striations and other imperfections that could probably be attributed to poor substrate quality. Some of the best converted films were produced later in the program using low-defect substrates. Substrates were cleaned prior to deposition according to the procedure outlined during the previous contract period with minor exceptions. B and A Electronic grade sulphuric acid obtained from Allied Chemical, and Spectrar grade isopropyl alcohol from Mallinkrodt Chemical Works were used in cleaning the polished substrates. Deionized water was doubly distilled to improve the cleaning procedure. In order to minimize substrate handling during cleaning, platinum wire cages were employed instead of tweezers.

6.3 Results and Discussion

6.3.1 Garnet

Magnetic garnets of the approximate composition $Gd_1 Er_2 Fe_{4.5} Ga_{0.5} O_{12}$ were studied exclusively during this program. This Super VIII garnet has a lattice constant which is compatible with $Gd_3 Ga_5 O_{12}$ and can be deposited epitaxially on a (111) $Gd_3 Ga_5 O_{12}$ substrate. The composition of the spray

powder and sprayed film was slightly rich in gallium and iron content in order to insure that the garnet film, formed subsequently during the conversion step, consisted of the desired composition and contained the desired properties.

6.3.2 Solvent

A flux of composition 50 parts PbO:1 part B_2O_3 by weight was used throughout this study. Oxide components, equivalent to the gallium-rich, iron-rich starting garnet composition, were combined with the flux oxides at elevated temperature and then cooled and converted into a homogeneous spray powder.

Since sprayed films contain only a small amount of garnet oxides and flux, the flux-to-garnet ratio is sensitive to small changes in the amount of flux such as that lost by evaporation. Therefore, closed crucibles were used during oxide fusion and closed boats were used during the conversion process to minimize flux evaporation.

6.3.3 Spraying Studies

Powders, containing garnet oxides and flux prepared as described earlier, were melted using a plasma torch and sprayed onto substrates to form deposits for subsequent conversion to the monocrystalline form. Three commercial spray torches were evaluated (Avco Model PG-100, Plasmadyne Model SG-3, and Plasmadyne Model SG-1B) and several powder feed mechanisms were investigated for processing this powder composition on GGG substrates. From a spray process variable study, the following

operating conditions were found to yield thin uniform coatings of flux and garnet components on cleaned substrates suitable for epitaxial conversion:

Spray Torch

Type	Plasmadyne, Model SG-1B (40 kw)
Arc Gas	Argon @ 60 cu. ft. /hr.
Arc current	150 amperes

Powder Feed Mechanism

Type	Plasmadyne Rotofeeder
Carrier Gas	Oxygen @ 15 cu. ft. /hr.

Other

Substrate preheat temp.	200°C
Torch-to-substrate dist.	4-1/2 inches

Sprayed films suitable for conversion were prepared in the thickness range of 2 to 15 mils. The magnetically characterized films shown later in Table VII , were 4 to 9 mils thick, as sprayed. When spraying was completed, coated substrates were removed from the spray station, placed in a closed platinum crucible, in a preheated furnace for prescribed thermal treatment and conversion.

6.3.4 Conversion Studies

The growth conditions used by Monsanto in the "dip" process were investigated initially with sprayed films in the two-step conversion process. These conditions consisted of : (1) a 2 to 4 hour homogenization of the individual oxides making up the garnet and the $PbO-B_2O_3$ flux at a temperature

of ~1050°C, and, (2) cooling to the growth temperature of 925°C to 935°C to form a supersaturated solution. However, changes in the growth cycle were required to convert sprayed deposits into monocrystalline films.

Prior to conversion, the plasma-sprayed film consists of a relatively homogeneous dispersion of the individual oxides in the flux on the surface of the GGG substrate. As the specimen is heated, the flux becomes molten at ~ 850°C and the garnet oxide components begin to dissolve. Due to the increasing temperature, no garnet deposition will take place. However, substrate attack by the flux will occur. It became evident that the long exposure time at the 1050°C homogenization temperature was resulting in excessive substrate attack. Therefore, the homogenization temperature and time were reduced according to the results of a brief statistical study. These changes improved the quality of converted films as shown in Table VI.

Because of the rapid quenching used in producing the spray powder, the garnet oxide components are present as a very fine dispersion in the flux. This feature allows the plasma-sprayed film to homogenize quickly and at a low temperature.

The effect of cooling rate from the homogenization temperature to the growth temperature was investigated. A fast cooling rate (~20°C/min.) from the homogenization temperature to just below the liquidus was found most suitable to minimize substrate etching. A slow cooling rate (~ 2.5°C/min.) from the liquidus to the growth temperature gave the best film quality.

TABLE VI

Effect of Homogenization Conditions on Quality of Converted Films

Specimen Number	Homogenization Temp. °C	Homogenization Time min.	Presence of Crystallites	Growth Surface	Domain width microns	Defect Density
149557-5	1032	10	orthoferrite and garnet	Frosted	20	High
149562-1	1035	2	orthoferrite and garnet	Frosted	--	High
149562-4	990	1	orthoferrite	Glossy	7	Low
149563-1	990	8	None	Glossy	40	Med.

Garnet films of comparable quality were successfully grown at growth temperatures between 925°C and 935°C. Growth rates of from 0.04 - 0.1 μm/minute were realized depending on growth temperatures.

Initial conversion experiments included tilting the furnace to decant the remaining flux and garnet from the grown film. However, the small amount of residual flux coupled with its high viscosity resulted in only partial decanting. Due to the small amount of flux involved it was decided to leave the flux in place and allow uniform film growth instead of "mesa" formation on those areas where flux might remain. However, the effect of the flux on film surface roughness was not determined.

A brief study was made to define the contribution of the plasma spraying process in forming candidate polycrystalline films for subsequent conversion to monocrystalline films. Reacted garnet plus flux powder, used in the plasma spraying of films for conversion, was wetted with isopropyl alcohol and the resulting paste was applied as a thin coating on GGG substrates. Coated substrates were subsequently heated in a manner similar to that used with plasma-sprayed films. Such films contained glossy surfaces and well-defined serpentine patterns. They also exhibited defects in the form of etch pits and apparent crystal pull-out or holes. The overall quality of the best converted powdered film was not as good as the best converted sprayed films prepared to date.

6.3.5 Characteristics of Selected Converted Films

All converted films were washed in dilute nitric acid to remove residual flux then examined microscopically for serpentine domain patterns

using polarized light. Film surface glossiness and the presence and types of second phases and defects were also noted. Five garnet films representative of those prepared by the two-step method of spraying and converting during this program were more critically analysed and these characterization data are summarized in Table VII. The conversion process conditions used in preparing these representative films are contained in Table VIII.

Thickness varied across each sprayed sample and better control of this property is needed. The thickness values tabulated for these selected samples were obtained over the most uniform area of the film. However, the low coercivity observed indicates that the GGG substrate surface was apparently not damaged by the process. The coercivity value observed in Run 24 was about as low as possible with this garnet system. The variation in $4\pi M_s$ among our samples might be due to variation in film composition, particularly gallium content, which could probably be traced to process variable changes made during film preparation. While none of these samples were of device quality, they were sent to the agency together with characterization data in order to meet the sample delivery schedule.

TABLE VII

Characterization Data of Selected Plasma-Sprayed and Converted Bubble Films

Sample Number	Conversion Run No.	h	ℓ	$4\pi M_s$	H_c	H_{s-b}	d_{s-b}	H_0	d_0	σ_w
APS 1	14	5.33	.51	259	0.26	117	6	143	2	.27
APS 2	24	2.98	.84	173	0.05	37	6	52	2	.20
APS 3	25	6.04	4.5	~46	~0.08	-	-	~ 4	-	-
APS 4	29	5.94	.88	133	-	40	10	60	3	.12
APS 5	31	2.17	.66	173	-	33	6	49	2	.15

Legend

h	Thickness, μm	H_c	Coercivity, Oe
ℓ	Characteristic Length, μm	H_{s-b}	Strip to Bubble Transition field, Oe
$4\pi M_s$	Saturation Magnetization, Gauss	d_{s-b}	Bubble diameter at H_{s-b}, μm
		H_0	Bubble collapse field, Oe
		d_0	Bubble diameter at H_0, μm
		σ_w	Domain wall energy/unit area, ergs/cm²

TABLE VIII

Process Conditions Used for Preparing Selected Representative Films by the Two-Step Method of Spraying and Conversion

Specimen Number	Conversion Run No.	Homogenization Hold Temp. °C	Homogenization Hold time, min.	Cooling Rates		Growth Conditions	
				to 150°C/min	From 950°C to growth temp. °C/min.	Temp. °C	Time, min.
APS1	14	1034	9	20	2	930	40
APS2	24	990	1	30	3	928	62
APS3	25	995	1.5	25	2	928	60
APS4	29	987	2	35	3	926	60
APS5	31	990	2	40	3	929	60

7. CHARACTERIZATION

7.1 Introduction

Reports issued during the preceding contract have dealt extensively with the characterization techniques in use in this work.[19, 20] Some improvements and corrections to existing techniques have been made and new measurements instituted. These new developments are discussed in this section.

7.2 Temperature Variation of Film Properties

Knowledge of the variations of bubble material properties with temperature is important in selecting materials for applications in which they will be subject to a range of temperatures. In general, constant operating bubble diameter at constant or slowly decreasing bias field is desirable. In terms of the basic materials parameters this translates to nearly constant characteristic length at constant or slowly decreasing magnetization[21]. These properties must be closely approximated while still maintaining the highest possible mobility, low coercivity, and reasonable anisotropy.

Variable temperature measurements are being made on materials for this contract by means of a thermoelectric unit adapted for use on a microscope stage. Figure 6A shows a cross-sectional view of this system. Its basis is the annular thermo-electric unit with water cooled reference side. The sample rests on a high thermal conductivity IRTRAN-5* plate in good contact with the variable temperature side. The unit is enclosed in

* Trade-name of the Eastman Kodak Co.

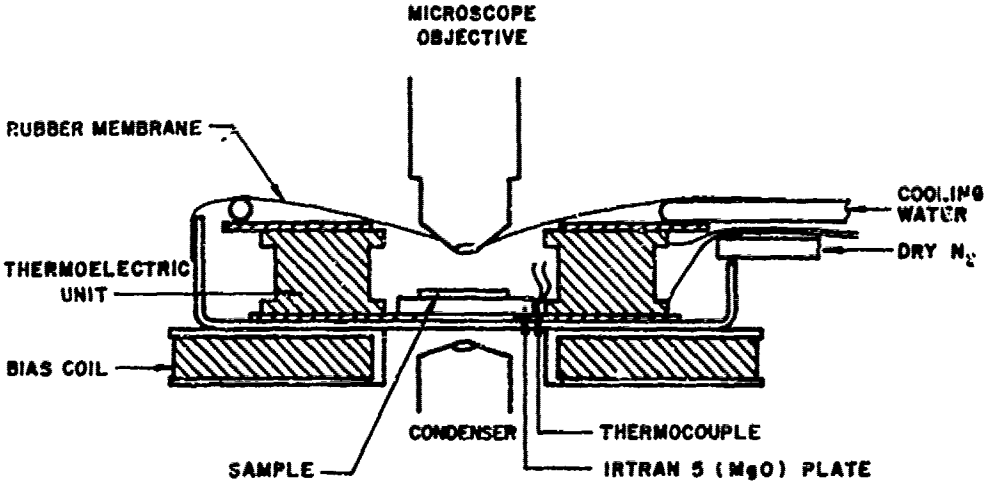

Figure 6A. Variable Temperature Stage - Cross Section

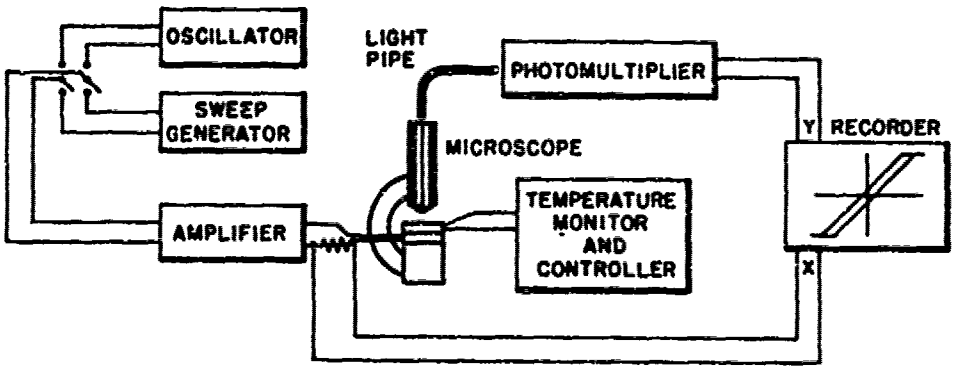

Figure 6B. Variable Temperature Hysteresis System

a glass housing topped with a rubber membrane to keep out moisture and thus reduce condensation and frost formation on the sample. In addition, dry nitrogen gas is brought into the housing for the same purpose. A hole is left in the rubber membrane for viewing purposes. This forms a reasonable seal against the objective lens housing when in position under the microscope.

The widely used technique of Fowlis and Copeland[22] for measurement of $4\pi M_s$ and ℓ requires that bubbles be formed for each measurement. As previously discussed, the preferred method for bubble formation from the normal strip domain pattern is cutting with a magnetic probe. Since access to the sample in the variable temperature stage is inconvenient, we are using the strip domain hysteresis measurement to determine $4\pi M_s$ and ℓ at various temperatures. The circuit block diagram is shown in Figure 6B. In order to establish an equilibrium array of parallel strips for the strip width measurement, the oscillator is used once temperature equilibrium has been established. When it is desired to record the hysteresis loop, the operational amplifier sweep generator is employed to drive the bias field around the complete loop. Normally, data are taken at approximately 0, 25, and 50°C and the average temperature coefficients determined over this range. The stage is capable of a temperature range from -20°C to + 80°C, however. Values of the temperature coefficients for LPE materials delivered under this and the preceding contract are presented in Table IX. It is clear from this table that the desired zero temperature coefficient for

TABLE IX

Values of characteristic length, ℓ, saturation magnetization, $4\pi M_s$, Neel temperature, T_N, and compensation temperature, T_c, together with temperature coefficients of ℓ, $4\pi M_s$, and domain wall energy density, σ_w, for various LPE garnet compositions.

Composition Number	ℓ μm	$4\pi M_s$ G	$\frac{100}{\ell}\frac{\Delta\ell}{\Delta T}$ %/°C	$\frac{100}{M_s}\frac{\Delta M_s}{\Delta T}$ %/°C	$\frac{100}{\sigma_w}\frac{\Delta\sigma_w}{\Delta T}$	T_N °C	T_c °C
$Eu_{.62}Er_{2.38}Fe_{4.41}Ga_{.59}O_{12}$	0.50	344	-0.95	+0.06	-0.83	181	-103
$Gd_{.8}Er_{2.2}Fe_{4.55}Ga_{.45}O_{12}$	0.57	213	-2.3	+0.65	-1.0	206	- 39
$Gd_{.46}Y_{2.54}Fe_{3.95}Ga_{1.05}O_{12}$	0.42	140	-0.91	+0.20	-0.51	133	-119
$Gd_{.99}Y_{1.15}Yb_{.86}Fe_{4.16}Ga_{.84}O_{12}$	0.48	170	-1.14	+0.14	-0.86	164	- 74
$Gd_{.3}Y_{2.53}La_{.17}Fe_{4.01}Ga_{.99}O_{12}$	0.70	117	-1.27	-0.27	-1.81	125	-127
$Gd_{.85}Tm_{1.3}Y_{.85}Fe_{4.2}Ga_{.8}O_{12}$	0.69	157	-2.41	+0.56	-1.29	178	- 68
$Eu_2Y_1Fe_{4.1}Al_{.9}O_{12}$	0.83	155	-0.73	-0.26	-1.30	130	< -195
$Eu_{0.4}Y_{2.6}Fe_{3.78}Ga_{1.22}O_{12}$	0.60	148	-0.63	-0.39	-1.41	123	< -195

has not yet been achieved. However, the EuY compositions can be expected to be useful in devices with finite operating margins over the 0 to 50°C range. Henceforth such results will be supplied with the characterization data for each material delivered.

7.3 Compensation Temperature

Also included in Table IX are values of T_c, the compensation temperature; that temperature at which the sum of the rare-earth and octahedral iron sublattice magnetizations just equal the tetrahedral iron sublattice magnetization yielding a net zero moment. A method very similar to that in use for Neel temperature measurements[23] has been us detect the compensation temperature. In it an AC field is used to modulate the domain pattern and the effect is optically detected via photomultiplier and lock-in amplifier. The octahedral sublattice dominates the Faraday rotation which therefore does not go to zero at compensation. However, the net magnetization reverses with respect to the sublattices at that temperature so that the optical signal is seen to pass through zero at T_c. The sample assembly is allowed to cool slowly in a partially filled Dewar vessel containing liquid nitrogen and the signal is monitored during cooling and later warming. When the zero of signal persists over a finite temperature range due to coercivity effects the center of the range is taken to be T_c. Such measurements, when all factors are considered, may be uncertain within a $\pm$ 4°C range.

7.4 Neel Temperature

An error in one of the charts used to determine Neel temperature has been found and the previously reported values corrected. These are

TABLE X

CORRECTED VALUES OF NEEL TEMPERATURE (T_N)

AND

ANISOTROPY FIELD (H_A)

Sample Number	T_N (K)	H_A (Oe)	Sample Number	T_N (K)	H_A (Oe)
EuEr-1	461	3800	GdYLa-1	399	450
EuEr-2	460	3800	GdYLa-2	399.5	450
EuEr-3	459	3800	GdYLa-3	398	450
EuEr-4	459	3800	GdYLa-4	398.5	450
EuEr-5	460	3800	GdYLa-5	399	450
EuEr-6	454	3800			
GdEr-1	478	1140	GdYTm-1	451	1000
GdEr-2	480	1360	GdYTm-2	451	1000
GdEr-3	479	1320	GdYTm-3	451	1000
GdEr-4	481	1180	GdYTm-4	451	1000
GdEr-5	479.5	1200	GdYTm-5	451	1000
GdY-1	405.5	220	EuY-1	404	1450
GdY-2	405	210	EuY-2	402	1550
GdY-3	404.5	230	EuY-3	402	1180
GdY-4	406	200	EuY-4	400	1130
GdY-5	405.5	220	EuY-5	402	1090
GdYYb-1	438	400	EuY-11	396	1180
GdYYb-2	438	430	EuY-12	396	1180
GdYYb-3	437	450	EuY-13	396	1180
GdYYb-4	437.5	480	EuY-14	396	1180
GdYYb-5	438	490	EuY-15	396	1180

also contained in Table IX for the particular representative samples selected for that table. The full set of corrected values for all samples delivered during the preceding contract is contained in Table X. Those values of T_N reported during the present contract have been free of this error.

It is informative to display the magnetization as a function of temperature using all of these data. Such plots are presented for representative samples of each composition in Figure 7. These curves show quite dramatically the undesirable temperature behavior of the GdEr and GdYTm compositions. They also suggest some interesting differences in shape of these curves from one composition to another. Particularly, GdYYb appears to be unusually sharply peaked while other compositions have their maxima skewed to high or low temperature (for example, GdY and GdYLa, respectively). At present, the data are too sparse to be more than suggestive of these variations. Further studies will be undertaken as time permits.

7.5 Anisotropy Field

One further correction to the characterization data should be mentioned. The theoretical interpretation of the magneto-optical anisotropy data was incomplete at the time that the characterization report was written. Since then the work of Shumate et al.[24] and the technique of Josephs[25] have become available. These form the basis for two new approaches to anisotropy and make clear that a correction is needed to our previous anisotropy field values. The details of these methods have been well presented by the respective authors and will not be repeated here. After some trial of each approach we have concluded that the high field susceptibility technique of

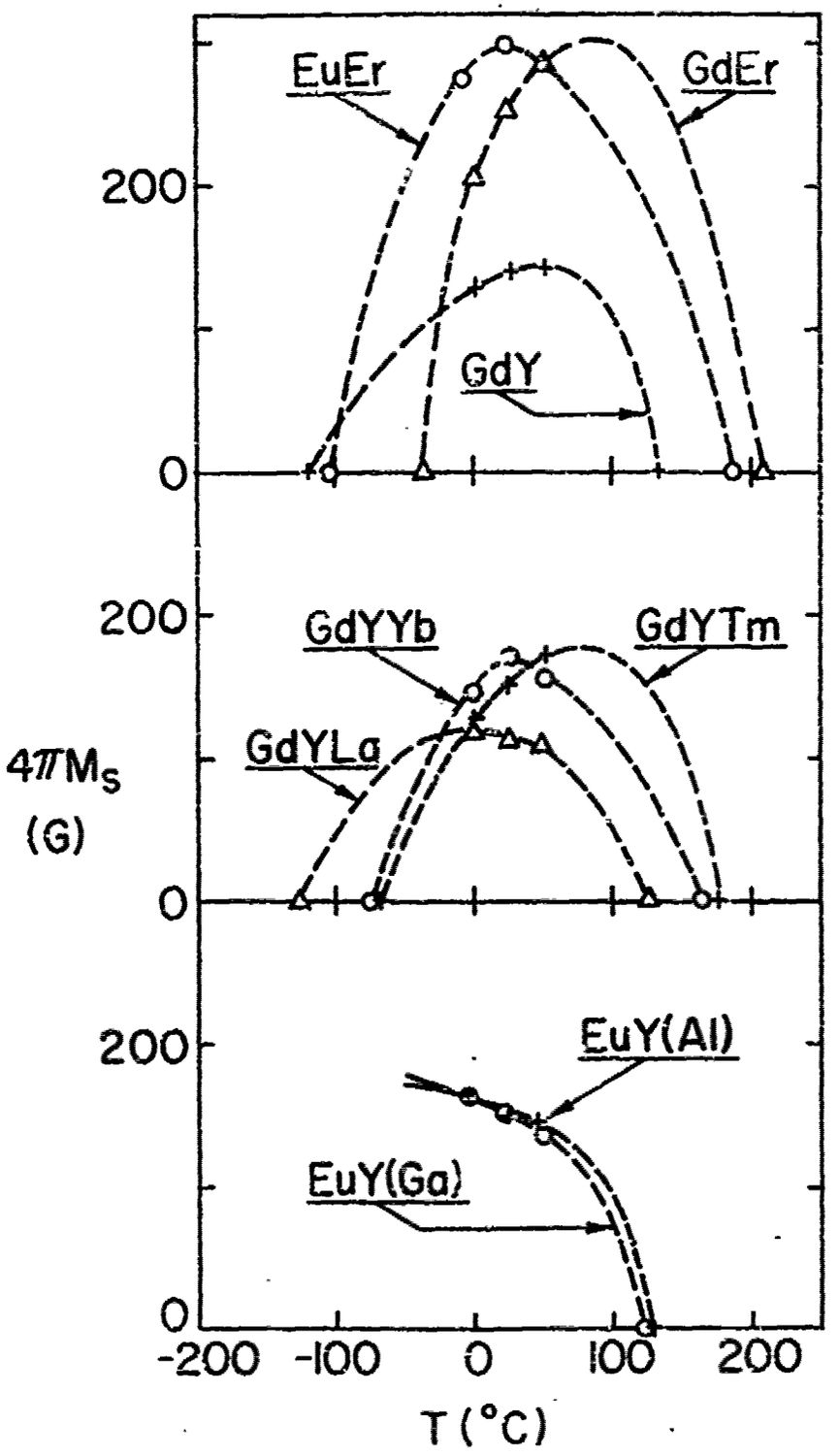

Figure 7. Magnetization versus Temperature for Various Garnet Film Compositions

Josephs is more immune to small misorientation errors and thus the better one for routine use. In addition, it also provides for comparison the wall susceptibility data which we have previously used while resting on a better theoretical base than that approach.

Values of anisotropy field, H_A, quoted for materials shipped prior to January 1, 1973, were based upon the maximum field at which wall susceptibility was observed, H_{WM}, to which $4\pi M_s$ was added (i.e. $H_A = H_{WM} + 4\pi M_s$). More careful analysis indicates that this addition of $4\pi M_s$, thought to arise from the demagnetizing factor for a plate sample, does not apply in this case. As the magnetization is pulled into the film plane by a strong field, the wall energy approaches zero (because of the small angel between M_s in adjacent domains) and the wall susceptibility can be expected to continue to approximately H_A. Thus the earlier values are too large by an amount comparable to $4\pi M_s$. This correction is generally less than the 10% uncertainty claimed for H_A but, as a systematic error, should be made. These corrections have been made in the values of H_A shown in Table X.

8. CONCLUSIONS

High quality boules of GGG have been grown under conditions which eliminate the highly strained central core and assure few dislocations and other defects. The interrelated effects of growth conditions on crystal quality is better understood. Work will continue on GGG, and SmGaG in an endeavor to further improve the crystalline quality and reproducibility.

In the LPE area work will continue on temperature stability and mobility improvement. Very likely layers of Pr^{3+}, Nd^{3+}, and/or Sm^{3+} substituted YGaIG will be investigated for future deliveries. This contract period has seen a dramatic improvement in the thickness uniformity of bubble materials. The procedures implemented to achieve this thickness uniformity will be defined further during the next report period.

Epitaxial films of Super VIII garnets were grown on GGG by a two-step process involving the plasma deposition of a film on a substrate followed by thermal conversion to a monocrystalline film.

Although the best films prepared within the available time were not of device quality, these studies did demonstrate that garnet films could be fabricated by the epitaxial conversion of plasma sprayed films.

During the next report period, a one-step process for achieving a single crystal bubble film by direct spraying will be investigated.

9. REFERENCES

1. J. W. Moody, R. M. Sandfort, and R. W. Shaw, "Final Report: Magnetic Bubble Materials," Contract No. DAAH01-72-C-0490 (August 1972).

2. C. D. Brandle, D. C. Miller, and J. W. Nielsen, "The Elimination of Defects in Czochralski Grown Rare- Earth Gallium Garnets," J. Cryst. Growth, 12, 195 (1972).

3. D. F. O'Kane and V. Sadagopan, "Crystal Growth and Characterization of Gadolinium Gallium Garnet," Paper No. 9 Electrochemical Society Meeting, Houston, Texas (May 1972).

4. H. L. Glass, "X-Ray Double Crystal Analysis of Facets in Czochralski Grown Gadolinium Gallium Garnet," Mat. Res. Bull. 7, 1087 (1972).

5. B. Cockayne, M. Cheswas, and D. B. Gasson, "The Growth of Strain Free $Y_3 Al_5 O_{12}$ Single Crystals," J. Mat. Sci., 3, 224 (1968).

6. T. S. Plaskett, E. Kokholm, H. L. Hu, and D. F. O'Kane, "Magnetic Bubble Domains in $(EuY)_3 Fe_5 O_{12}$ Films on $Sm_3 Ga_5 O_{12}$ Substrates," Paper 3D-4 18th Ann. Conf. on Magnetism and Magnetic Materials, Denver, Colo. (Nov. 1972).

7. J. W. Nielsen, "Growth of Garnet Substrates and Epitaxial Films for Bubble Devices," AIP Conference Proceedings No. 5, 56 (1972).

8. W. H. Von Aulock, Handbook of Microwave Ferrite Materials, Academic Press., New York, 1965.

9. F. B. Hagedorn, W. F. Tabor, J. E. Geusic, H. J. Levinstein, S. J. Licht, and L. K. Schick, "Cylinderical Magnetic Domain Epitaxial Film Characterization: Device and Growth Implications," Appl. Phys. Ltrs. 19, 95 (1971).

10. D. H. Smith and A. W. Anderson, "The temperature Dependence of Bubble Parameters in Some Rare-Earth Garnet Films," AIP Conference Proceedings No. 5, 120 (1972).

11. E. A. Giess, J. D. Kuptsis, and E. A. D. White, "Liquid Phase Epitaxial Growth of Magnetic Garnet Films by Isothermal Dipping in a Horizontal Plane with Axial Rotation," J. Cryst. Growth, 16, 36 (1972).

12. R. C. Linares and R. B. McGraw, Jr., "Vapor Growth of Yttrium Iron Garnet," J. Appl. Phys. 35, 3630 (1964).

13. R. C. Linares, R. B. McGraw, Jr., and J. B. Schroeder, "Growth and Properties of Yttrium Iron Garnet Single-Crystal Films," J. Appl. Phys. 36, 2884 (1964).

14. M. Robinson, A. H. Bobeck, and J. W. Nielsen, "Chemical Vapor Deposition of Magnetic Garnet for Bubble-Domain Devices," IEEE Trans. on Magn. MAG 4 , 464 (1971).

15. B. F. Stein, "Growth and Some Magnetic Properties of GdIG Films," J. Appl. Phys. 42, 2336. (1971).

16. S. T. Ospresko and H. L. Pinch, "Control of Product Phase in the Chemical Vapor Deposition of Garnet Films," Mat. Res. Bull. 7, 685 (1972).

17. R. C. Taylor and V. Sadagopan, "Growth of Uniaxial Magnetic Garnet Films by a Simplified Method of Chemical Vapor Deposition," Appl. Phys. Ltrs., 19, 361 (1971).

18. F. H. Wehmeier, "General Thermodynamic Considerations for the Chemical Transport of Ternary Compounds; Chemical Transport of Yttrium Iron Garnet with HCl", J. Cryst. Growth, 6, 341 (1970).

19. R. W. Shaw, R. M. Sandfort, and J. W. Moody, Magnetic Bubble Materials: Initial Characterization Report Contract No. DAAH01-72-C-0490 (March, 1972)

20. R. W. Shaw, R. M. Sandfort, and J. W. Moody, Magnetic Bubble Materials: Characterization Techniques Study Report, Contract No. DAAH01-72-C-0490 (July, 1972).

21. See, for example A. A. Thiele, J. Appl. Phys., 41, 1139 (1970).

22. D. C. Fowlis and J. A. Copeland, "Rapid Method for Determining the Magnetization and Intrinsic Length of Magnetic Bubble Domain Materials," AIP Conference Proceedings No. 5, 240 (1972).

23. Reference 19, pg. 39.

24. P. W. Shumate, Jr., D. H. Smith, and F. B. Hagedorn, "The Temperature Dependence of the Anisotropy Field and Coercivity in Epitaxial Films of Mixed Rare-Earth Iron Garnets," J. Appl. Phys.1, 44, 449 (1973)

25. R. M. Josephs, " Determination of the Physical Parameters Characterizing the Magnetic Behavior of Bubble Domains, " Paper 2C-4, 18th Annual Conference on Magnetism and Magnetic Materials, Denver, Colo. (Nov. 1972).